The Bondi k-Factor as Quantum Operator: A Two-Sector Decomposition of the Lorentz Transformation

Badriram Rajagopalan
Independent Researcher
ORCID: 0009-0000-1858-5471

April 25, 2026

Abstract

We promote the Bondi k-factor to an operator $\hat{k} = (\hat{H}_{\rm cm} + \hat{p}c)/(mc^2)$ and prove that the Lorentz transformation decomposes into two sectors with structurally distinct quantum behavior: a time dilation sector $\hat{k} + \hat{k}^{-1} = 2\hat{E}/(mc^2)$, nonlinear in momentum, and a simultaneity sector $\hat{k} - \hat{k}^{-1} = 2\hat{p}c/(mc^2)$, linear in momentum.

The asymmetry is proved via Jensen's inequality. Rest mass $m > 0$ bounds the energy spectrum below, making $E(p)$ strictly convex. Convexity simultaneously produces Jensen corrections, Pikovski decoherence, and the Pauli obstruction — all confined to the time dilation sector. The simultaneity sector is protected exactly by linearity. The decomposition is universal across physically distinct clock types (light-bounce, radioactive decay, gravitational pendulum): which sector produces corrections and which is protected is independent of the clock mechanism.

The decomposition provides a structural explanation for the angular separation of the quantum corrections computed by Grochowski et al. [14]: the time dilation sector and the simultaneity sector map onto their "quantum time dilation" and "quantum Doppler shift" contributions, separable by angular detection geometry. The framework does not predict these corrections but organizes them under a single structural cause. All corrections vanish in the classical limit $\sigma_p \to 0$, recovering the Bondi derivation of Part I [1] exactly. The axiomatic and categorical foundations are developed in Part II [2].

1. Context

1.1. The Bondi–$N_{\rm ref}$ result

Part I [1] derives the full Lorentz transformation from three operational inputs: transition-count ratios between inertial observers ($N_{\rm ref}$), the relativity principle, and a finite signal speed c. The derivation uses Bondi's k-calculus (1964) [8], reframed as the natural formalism for the surplus structure framework; no prior notion of time, metric, or spacetime is assumed, and $1/\gamma$ emerges as a theorem rather than an input. The k-factor — the ratio of receiver's count at reception to sender's count at emission — is:

$$k = \sqrt{(1+\beta)/(1-\beta)}$$

and the Lorentz transformation follows from two algebraic identities:

$$k + 1/k = 2\gamma \quad \text{(time dilation sector)}$$

$$k - 1/k = 2\beta\gamma \quad \text{(simultaneity sector)}$$

The derivation is kinematic — it uses sharp positions, sharp momenta, sharp clock readings. This paper asks: what happens when the clocks are quantum? The axiomatic and categorical foundations are given in Part II [2].

1.2. What this paper does

Six things, in order:

1. **PaW grounding (§§2–3):** Maps the Bondi ingredients onto the Page–Wootters framework and extracts k as a ratio of clock POVM eigenvalues. Completes the chain from $\hat{H}|\Psi\rangle = 0$ to the full Lorentz transformation.

2. **Quantum corrections (§4):** Promotes k to an operator, computes corrections for a detector in a momentum superposition, and identifies the asymmetry between the time dilation and simultaneity sectors.

3. **Bondi decomposition of the proper time (§5):** Shows that the standard proper time $\omega_0 Lm/p$ separates into time dilation and simultaneity contributions under the k-operator algebra, with different quantum-correction profiles. Clarifies the structure of the Pikovski decoherence mechanism.

4. **The sector asymmetry, structurally (§6):** Proves via Jensen's inequality that strict convexity of $E(p)$ for $m > 0$ confines all quantum corrections (Jensen, Pikovski, Pauli, Grochowski) to the time dilation sector, leaving the simultaneity sector exactly protected by linearity.

5. **Universal sector structure (§§8–9):** Shows that the two-sector decomposition is constrained by quantum Fisher information and applies to all clock types (light-bounce, radioactive decay, gravitational pendulum), with the structure — which sector produces corrections and which is protected — independent of the clock mechanism.

6. **Experimental connections (§§7, 10, 11.3):** Maps the sector decomposition onto the Grochowski et al. spectroscopy result [14] and the Pikovski decoherence mechanism, and discusses prospects with the Covey–Pikovski–Borregaard distributed atomic clock proposal [19].

2. PaW Substitution: From Bondi to Quantum Clocks

2.1. The substitution map

Each Bondi ingredient has a PaW counterpart:

A note on the mass-shell constraint. The mass-shell relation $E^2 = p^2c^2 + m^2c^4$ is not an independent assumption importing Lorentz invariance. It is the unique Casimir invariant of the Poincaré group, which itself follows from a finite speed limit c plus homogeneity, isotropy, and group closure (Ignatowsky 1910 [12]; Berzi & Gorini 1969 [13]). The empirical inputs are: one number — c — and the identification of the system as a massive particle (i.e., that it transforms as a massive representation of the resulting symmetry group). Given these, the Lorentzian signature and the mass-shell relation are derived consequences.

2.2. The model

Hilbert space. $\mathcal{H} = \mathcal{H}_{C_1} \otimes \mathcal{H}_{C_2} \otimes \mathcal{H}_F$, where C_1 (observer P) and C_2 (observer T) are massive composite particles with internal Hamiltonians $\hat{H}_{0i}$ and center-of-mass degrees of freedom, and F is a massless scalar field mediating signals. The model is $1+1$ dimensional.

The constraint. The global state satisfies $\hat{H}|\Psi\rangle = 0$, where:

$$\hat{H} = \hat{C}_1 + \hat{C}_2 + \hat{H}_F + \hat{H}_{\text{int}}$$

Each clock's mass-shell constraint (Smith & Ahmadi 2020 [4]):

$$\hat{C}_i = p_{t,i}^2 - p_{x,i}^2 c^2 - m_i^2 c^4 - 2m_i c^2 \hat{H}_{0i} = 0$$

Deparametrized using particle i's internal clock:

$$\hat{H}_{\text{eff,i}} = \gamma_i m_i c^2 + \hat{H}_{0i}/\gamma_i$$

Clock observables. Following Höhn, Smith & Lock (2021, relativistic settings) [6], each clock's time is given by a covariant POVM E_{C_i} transforming covariantly with respect to the clock's quadratic Hamiltonian. The POVM outcomes are the clock readings τ_i.

2.3. Extracting the k-factor from PaW eigenvalues

Initial conditions. At the co-location event, both clocks read zero: $\tau_1 = \tau_2 = 0$, $x_1 = x_2 = 0$. After this, C_2 moves at velocity ratio β relative to C_1.

Step 1. Condition on C_1's clock reading τ_1. C_2's position: $x_2 = \beta\tau_1$ (light-transition units). C_2's clock reading: $\tau_2 = \tau_1/\gamma$ (mass-shell suppression, established by the Trinity equivalence [5]).

Step 2. C_1 emits a signal — a field excitation propagating at $c = 1$ (massless sector of the constraint).

Step 3. Signal propagation. Spatial gap at emission: $\beta\tau_1$. Closing speed: $(1-\beta)$. Signal arrives at C_1-time $\tau_1/(1-\beta)$.

Step 4. C_2's POVM eigenvalue at arrival: $\tau_2(\text{arrival}) = \tau_1/((1-\beta)\gamma)$.

Step 5. The k-factor:

$$k = \tau_2(\text{arrival})/\tau_1(\text{emission}) = 1/((1-\beta)\gamma)$$

Evaluating: $(1-\beta)\gamma = \sqrt{(1-\beta)/(1+\beta)}$. Therefore:

$$k = \sqrt{(1+\beta)/(1-\beta)}$$

This is the Bondi k-factor, now derived as a ratio of PaW clock POVM eigenvalues. The decomposition $k = (1+\beta)\gamma$ separates signal propagation ($1+\beta$, from the field subsystem) from tick rate suppression (γ, from the mass-shell constraint).

Verification. The return signal gives $\tau_1(\text{echo}) = k^2\tau_1$, and the ratio $\tau_1(\text{echo})/\tau_2(\text{re-emission}) = k$ — confirming the symmetry guaranteed by the perspective-neutral structure.

3. The Derivational Chain

The complete chain, from PaW constraint to full Lorentz transformation:

- $\hat{H}|\Psi\rangle = 0$ (PaW global constraint)
- Mass-shell condition for each clock subsystem (Smith & Ahmadi 2020)
- $1/\gamma$ tick rate suppression of internal dynamics (Pikovski $\hat{H}_0/\gamma$)
- Field propagation at c (massless sector of constraint)
- k-factor as ratio of clock POVM eigenvalues: $k = \sqrt{(1+\beta)/(1-\beta)}$
- Bondi algebra: $k + 1/k = 2\gamma$, $k - 1/k = 2\beta\gamma$
- Full Lorentz transformation: $t' = \gamma(t - vx/c^2)$, $x' = \gamma(x - vt)$

No temporal manifold, Minkowski metric, or synchronization convention were assumed as input. Spatial positions enter operationally through radar measurements. The mass-shell relation is derived from the finite speed limit plus homogeneity, isotropy, and group closure (Ignatowsky 1910 [12]; Berzi & Gorini 1969 [13]). The Lorentz transformation is the output of the PaW constraint structure.

The computation in §2.3 uses the classical limit — definite positions, definite clock readings, definite signal trajectories. The classical limit is appropriate for deriving the Lorentz transformation, which is itself a classical statement. What follows extends to the quantum regime.

3.1. Relation to standard relativistic atom interferometry

The standard treatment of relativistic atom interferometry (Bordé 1989, Dimopoulos et al. 2008) computes the phase accumulated along each arm using the relativistic action $S = \int L\, d\tau$, where the Lagrangian contains the time dilation factor γ. The proper-time integral gives $\omega_0\tau = \omega_0 Lm/p$ for an atom with momentum p traversing baseline L.

The k-operator decomposition (§4) reveals the internal structure of this proper time. Under the Bondi algebra, the proper time decomposes into two sectors:

- Time dilation sector: $\omega_0(Lm/p + Lp/(mc^2))$ — contains both the leading $1/p$ term and a $+p$ correction

Bondi ingredient	PaW counterpart	Established by	Status
Clock reading (N_{ref})	Clock POVM eigenvalue	Page & Wootters (1983) [7]; Höhn, Smith & Lock (2021) [5, 6]	Direct substitution
Tick rate suppression ($1/\gamma$)	Mass-shell constraint deparametrized $= \hat{H}_0/\gamma$	Smith & Ahmadi (2020) [4]	Direct substitution
Maximum signal speed (c)	Structural constant of the mass-shell constraint	Constraint implies Lorentzian causal ordering	Established
Observer-independence of c	Same constraint for all deparametrizations	Universality of $\hat{H}\|\Psi\rangle = 0$	Established
Two spatially separated observers	Two clock subsystems with translational DOF	Vanrietvelde, Höhn & Giacomini (2023) [10]	Established
Signal propagation	Field excitation between clock subsystems	Computed in §2.3	Computed below
k-factor	Ratio of clock POVM eigenvalues	Computed in §2.3	Computed below
Symmetry of k	Perspective-neutral structure	Vanrietvelde, Höhn & Giacomini (2020) [9]	Structurally guaranteed
Algebra: k → Lorentz transformation	Framework-independent	Bondi (1964) [8]	No gap

- Simultaneity sector: $-\omega_0 Lp/(mc^2)$ — a linear-in-p contribution with opposite sign

These sum to $\omega_0 Lm/p$ — the standard proper-time result. The action-based calculation delivers the total; the k-operator decomposition reveals the two-sector structure within it. The simultaneity sector is not absent from the action formalism — it is contained in the proper time that the action delivers. The k-operator makes the decomposition explicit.

4. The Quantum Extension: The k-Factor as Operator

4.1. The k-operator

When C_2 is in a momentum superposition, with state $\int dp\, f(p)\,|p\rangle \otimes |\phi_0\rangle$, the k-factor becomes an operator diagonal in the momentum basis (Figure 1):

$$\hat{k}\,|p\rangle = k(p)\,|p\rangle$$

Using $E = \sqrt{p^2c^2 + m^2c^4}$ and the identity $(E+pc)(E-pc) = m^2c^4$:

$$\hat{k} = \frac{\hat{H}_{\text{cm}} + \hat{p}c}{mc^2}, \qquad \hat{k}^{-1} = \frac{\hat{H}_{\text{cm}} - \hat{p}c}{mc^2}$$

The k-factor is the forward light-cone momentum divided by the rest energy. The two combinations entering the Lorentz transformation are:

$$\hat{k} + \hat{k}^{-1} = \frac{2\hat{H}_{\text{cm}}}{mc^2} = 2\hat{\gamma} \qquad \text{(time dilation sector)}$$

$$\hat{k} - \hat{k}^{-1} = \frac{2\hat{p}c}{mc^2} \qquad \text{(simultaneity sector)}$$

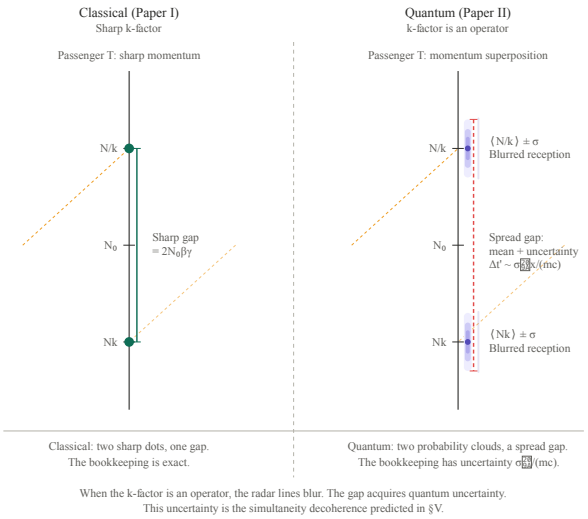

Figure 1: The k-operator in a blurred-radar diagram, extending Part I's Einstein-train illustration to the quantum regime. **Left:** classical case — passenger T has sharp momentum; the two signal receptions are sharp points on T's count axis, and the gap between them is a precise bracket. **Right:** quantum case — T carries a momentum superposition, each eigenvalue of $\hat{k}$ produces a different reception count, and the sharp points become probability distributions. The gap acquires quantum uncertainty $\Delta t' \sim \sigma_p x/(mc)$.

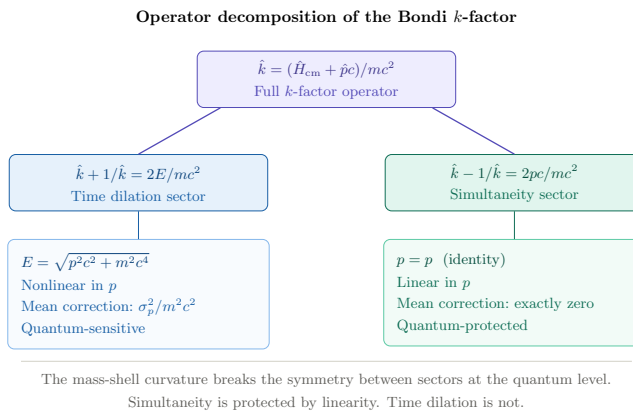

Figure 2: Operator decomposition of the k-factor into a time dilation sector $\hat{k}+\hat{k}^{-1}=2\hat{E}/(mc^2)$, nonlinear in momentum and acquiring all quantum corrections (Jensen, Pikovski, Pauli, Grochowski), and a simultaneity sector $\hat{k}-\hat{k}^{-1}=2\hat{p}c/(mc^2)$, linear in momentum and protected from corrections. The asymmetry is a consequence of the strict convexity of $E(p)$ for $m>0$ (Section 6).

4.2. The asymmetry: linearity protects simultaneity

The simultaneity sector ($\hat{k}-\hat{k}^{-1}=2\hat{p}c/(mc^2)$) is linear in p and therefore receives no quantum corrections for any symmetric wavepacket. The time dilation sector ($\hat{k}+\hat{k}^{-1}=2\hat{E}/(mc^2)$) is nonlinear in p and acquires corrections of order $\sigma_p^2/(m^2c^2)$ (Figure 2). The structural proof of this asymmetry, via Jensen's inequality applied to the strict convexity of $E(p)$, is given in Section 6.

4.3. Measurement statistics of the Lorentz transformation

The Lorentz transformation is exact — the symmetry group is not modified. What acquires quantum corrections is the measurement statistics of frame-dependent quantities when the detector is a quantum system with momentum spread σ_p. For a Gaussian momentum wavepacket centered on p_0 with spread σ_p:

Expectation values:

$$\langle t'\rangle = \gamma_0(t_P - \beta_0 x_P) + t_P\cdot\sigma_p^2/(2\gamma_0^3 m^2c^2)$$
$$\langle x'\rangle = \gamma_0(x_P - \beta_0 t_P) + x_P\cdot\sigma_p^2/(2\gamma_0^3 m^2c^2)$$

The corrections act as a uniform rescaling: $\gamma_{\rm eff}=\gamma_0(1+\sigma_p^2/(2\gamma_0^4m^2c^2))$. The simultaneity term $(-\beta_0 x_P)$ receives **no correction**.

Quantum uncertainties:

$$\Delta t' = \sigma_p/(mc)\times|\beta_0 t_P - x_P|$$
$$\Delta x' = \sigma_p/(mc)\times|\beta_0 x_P - t_P|$$

Both scale linearly with $\sigma_p/(mc)$ and grow with the radar separation between events.

4.4. The correspondence limit

The measurement statistics of §4.3 must reduce to the classical Bondi result of Part I [1] in the limit $\sigma_p\to 0$ (sharp momentum). Verification:

Mean corrections vanish. The time dilation correction $t_P\cdot\sigma_p^2/(2\gamma_0^3m^2c^2)\to 0$ as $\sigma_p\to 0$. The simultaneity correction is already zero for symmetric wavepackets at any σ_p. In the sharp-momentum limit, $\langle t'\rangle\to\gamma_0(t_P-\beta_0x_P)$ and $\langle x'\rangle\to\gamma_0(x_P-\beta_0t_P)$ — the exact classical Lorentz transformation.

Quantum uncertainties vanish. $\Delta t'=\sigma_p/(mc)\times|\beta_0t_P-x_P|\to 0$ and $\Delta x'=\sigma_p/(mc)\times|\beta_0x_P-t_P|\to 0$. The transformed coordinates become sharp — a single Lorentz frame, not a superposition of frames.

The k-factor becomes a number. As $\sigma_p\to 0$, the momentum distribution $f(p)\to\delta(p-p_0)$, the operator $\hat{k}$ collapses to its eigenvalue $k(p_0)=\sqrt{(1+\beta_0)/(1-\beta_0)}$, and the Bondi algebra of Part I [1] applies without modification.

Macroscopic detectors. For any macroscopic object ($m\gg$ atomic mass, $\sigma_p/(mc)\approx 0$), all quantum corrections are negligible. GPS satellites, LIGO mirrors, fiber-optic detectors — all operate deep in the correspondence limit where the classical Bondi derivation is exact. The quantum corrections are relevant only in the regime $\sigma_p/(mc)\gtrsim 10^{-11}$ (cold atoms at μK temperatures).

5. The Bondi Decomposition of the Proper Time

5.1. Two-sector structure

The proper time for an atom with momentum p traversing baseline L is $\tau=Lm/p$. The internal phase is $\omega_0\tau=\omega_0Lm/p$. Under the Bondi decomposition, this separates into contributions from the two sectors of the k-operator:

The simultaneity sector contributes twice the magnitude of the net relativistic correction, with opposite sign to the time dilation sector's $+p$ component. The net correction is $-\omega_0Lp/(2mc^2)$ — the standard second-order Doppler shift. The Bondi decomposition does not predict a new observable: the total phase ω_0Lm/p is the standard result, and any measurement of the interferometric phase will yield this total. The decomposition reveals *why* the second-order Doppler shift has the coefficient it does — it is the net of two opposing contributions from the two sectors.

5.2. The sector asymmetry under quantum averaging

The decomposition exhibits the asymmetry already flagged in §4.2. The simultaneity sector ($-\omega_0Lp/(mc^2)$) is linear in p; its mean receives no quantum corrections from momentum spread for any symmetric distribution. The time dilation sector ($\omega_0(Lm/p+Lp/(mc^2))$) contains the nonlinear $1/p$ term. Since $1/p$ is strictly convex for $p>0$, Jensen's inequality gives $\langle 1/p\rangle > 1/\langle p\rangle$: the ensemble-averaged proper time is longer than the proper time at the mean momentum. The structural proof and four corollaries are in Section 6.

5.3. Physical distinguishability of the sectors

The two sectors map onto experimentally distinguishable signatures in atomic spectroscopy already computed in the literature, separable by angular detection geometry. The full treatment — the identification of the sectors with the Grochowski et al. quantum time dilation and quantum Doppler corrections [14] — is given in Section 7.

Sector	Contribution	p-dependence	Magnitude (leading order)
Time dilation $(k+1/k)$	$\omega_0(Lm/p+Lp/(mc^2))$	Mixed: $1/p$ and $+p$	Dominant
Simultaneity $(k-1/k)$	$-\omega_0 Lp/(mc^2)$	Linear: $-p$	Twice the net correction
Total (proper time)	$\boldsymbol{\omega_0 Lm/p}$	$\boldsymbol{1/p}$	**Standard result**

6. The Sector Asymmetry: Structural Origin

The two sectors of the k-operator decomposition behave differently under quantum averaging. This section proves that the asymmetry is structural — a theorem of the mass-shell constraint — not a contingent feature of any particular clock.

6.1. Root cause: rest mass and convexity

Lemma 6.1 (Root cause of the sector asymmetry)**.** *Let $E(p)=\sqrt{p^2c^2+m^2c^4}$ be the relativistic energy. Then:*

1. *$\sigma(\hat{E})\subseteq[mc^2,\infty)$ — the spectrum of $\hat{E}$ is bounded below by $mc^2>0$.*
2. *$E(p)$ is strictly convex: $d^2E/dp^2=m^2c^6/E^3>0$ for all p.*
3. *$p\mapsto pc$ is linear: $d^2(pc)/dp^2=0$.*

The common cause of (i)–(iii) is rest mass $m>0$: it provides the scale that bounds the spectrum below and makes $E(p)$ bend away from linearity.

Proof. (i) $E(p)=\sqrt{p^2c^2+m^2c^4}\geq mc^2$ with equality iff $p=0$. (ii) $dE/dp=pc^2/E$; $d^2E/dp^2=m^2c^6/E^3>0$ since $E\geq mc^2>0$. (iii) Immediate. All three follow from $m>0$. □

6.2. The sector asymmetry via Jensen's inequality

Proposition 6.2 (Sector asymmetry)**.** *Let $f(p)$ be a symmetric momentum distribution centered on p_0 with spread σ_p. Then:*

1. ***Simultaneity sector is protected.*** *$\hat{k}-\hat{k}^{-1}=2\hat{p}c/(mc^2)$ is linear in $\hat{p}$. For any symmetric distribution:*

$$\langle\hat{k}-\hat{k}^{-1}\rangle=\frac{2\langle p\rangle c}{mc^2}=\frac{2p_0c}{mc^2}$$

exactly, with zero correction at any order in σ_p.

2. ***Time dilation sector acquires corrections.*** *$\hat{k}+\hat{k}^{-1}=2E(\hat{p})/(mc^2)$ where $E(p)$ is strictly convex. By Jensen's inequality:*

$$\langle E(\hat{p})\rangle>E(\langle\hat{p}\rangle)=E(p_0)$$

For a Gaussian wavepacket the leading correction is:

$$\langle\hat{k}+\hat{k}^{-1}\rangle=2\gamma_0+\frac{\sigma_p^2}{\gamma_0^3m^2c^2}+\mathcal{O}(\sigma_p^4)$$

Proof. (i) Linearity of $\hat{p}$ means $\langle\hat{p}\rangle=p_0$ exactly for any symmetric distribution. (ii) $E(p)$ satisfies $d^2E/dp^2>0$ strictly (Lemma 6.1), so Jensen's inequality applies. The leading correction follows from Taylor expansion of E around p_0. □

6.3. Four corollaries of the convexity

Corollary 6.3 (Jensen correction — time dilation sector)**.** *For any non-degenerate momentum distribution centered on p_0: $\langle E(\hat{p})\rangle>E(\langle\hat{p}\rangle)=E(p_0)$. The simultaneity sector satisfies $\langle\hat{p}c\rangle=p_0c$ exactly with zero correction.*

Corollary 6.4 (Pauli obstruction — time dilation sector only)**.** *No self-adjoint time operator can be canonically conjugate to $\hat{E}$, since $\sigma(\hat{E})\subseteq[mc^2,\infty)$ triggers Pauli's theorem [20]. Position $\hat{x}$ is canonically conjugate to $\hat{p}$ with no spectral obstruction, since $\sigma(\hat{p})=\mathbb{R}$.*

Corollary 6.5 (Pikovski decoherence — time dilation sector only)**.** *Momentum-spread dephasing of internal clocks originates from the time dilation sector. The phase spread is $\mathrm{Var}(\phi)\approx(\omega_0T)^2m^2c^8p_0^2/E(p_0)^6\cdot\sigma_p^2$, proportional to $(d\phi/dp)^2\sigma_p^2$. The simultaneity sector contributes no phase spread since $d(pc)/dp=c$ is constant [3].*

Corollary 6.6 (Grochowski angular separation)**.** *The quantum time dilation correction scales as $\mathcal{O}(v^2/c^2)$ and modifies the total decay rate; the quantum Doppler correction scales as $\mathcal{O}(v/c)$ and is angularly asymmetric. These map to the time dilation and simultaneity sectors respectively [14].*

6.4. Pauli-sector duality

All four corollaries trace to Lemma 6.1: rest mass $m>0$ bounds $\sigma(\hat{E})$ below, making $E(p)$ strictly convex, simultaneously producing the Jensen corrections, Pikovski decoherence, Grochowski angular separation, and the Pauli obstruction. The simultaneity sector evades all four because $\sigma(\hat{p})=\mathbb{R}$ and $p\mapsto pc$ is linear. The asymmetry between the sectors is a theorem of the mass-shell constraint, not an additional assumption.

The $(\hat{k}+\hat{k}^{-1},\,\hat{k}-\hat{k}^{-1})$ partition is distinguished by the property that one component is exactly linear in momentum and the other is not. Whether this is the unique decomposition with this property — or whether alternative partitions of functions of $\hat{k}$ could yield similar protection — is an open question.

7. Physical Distinguishability: Grochowski Spectroscopy

The sector decomposition is not merely a formal partition. Grochowski, Smith, Dragan, and Dębski [14] identified two physically distinct quantum corrections to relativistic atomic spectra that map directly onto the two sectors.

For a hydrogen-like atom in a coherent superposition of relativistic momentum states, two quantum corrections to spontaneous emission arise:

Quantum time dilation ($\mathcal{O}(v^2/c^2)$): modifies the total decay rate and depends on the second moment of the momentum distribution. This maps onto the time dilation

sector $\hat{k}+\hat{k}^{-1}=2\hat{E}/(mc^2)$. The correction is a direct consequence of Jensen's inequality applied to the nonlinear $E(p)$.

Quantum Doppler shift ($\mathcal{O}(v/c)$): modifies the spectral line shape but integrates to zero in its effect on the total decay rate. It is linear in momentum and maps onto the simultaneity sector $\hat{k}-\hat{k}^{-1}=2\hat{p}c/(mc^2)$.

The two corrections are separable by detection geometry: perpendicular detection ($\Theta=\pi/2$) isolates the time dilation sector; parallel detection ($\Theta=0$) is dominated by the simultaneity contribution. The k-operator decomposition is the structural explanation for why these corrections have the specific scaling and angular properties they do.

The angular separation is a consequence of the sector algebra, not a contingent feature of hydrogen. Any composite quantum system with rest mass $m>0$ in a momentum superposition will exhibit the same partition: nonlinear corrections from the time dilation sector, accessible at $\Theta=\pi/2$, and linear corrections from the simultaneity sector, dominant at $\Theta=0$.

The mapping is an identification: the two quantum corrections computed by Grochowski et al. have the same momentum scaling and angular dependence as the two k-operator sectors. The k-operator framework did not predict these corrections; it provides a structural explanation for why they have the properties they do.

8. Resource Exclusion: The QFI Criterion

Beyond the Grochowski signatures, the k-operator framework also constrains which quantum states can serve as clocks at all. The criterion is provided by quantum Fisher information.

Proposition 8.1 (QFI excludes dephased states from the clock resource)**.** *Let ρ be a state of a composite system evolving under $\hat{H}_{\text{phys}}=\hat{H}_0/\gamma$. If ρ is diagonal in the energy eigenbasis of $\hat{H}_{\text{phys}}$, then the quantum Fisher information $F_Q=4\,\text{Var}(\hat{H}_{\text{phys}})=0$ and the state cannot function as a clock.*

Proof. For ρ diagonal in the eigenbasis of $\hat{H}_{\text{phys}}$, coherences vanish and the evolved state $e^{-i\hat{H}_{\text{phys}}n}\rho\, e^{i\hat{H}_{\text{phys}}n}=\rho$ for all n — no clock phase accumulates. The quantum Cramér–Rao bound $(\Delta N_{\text{ref}})^2\geq 1/F_Q$ with $F_Q=0$ implies $\Delta N_{\text{ref}}=\infty$ — the clock parameter is unresolvable. Dephased states are automatically excluded from the clock resource. □

The QFI criterion connects to the resource theory of clocking capacity defined in Part II [2]. States with $F_Q=0$ are free states in the resource theory: they carry no asymmetry under time translations and cannot distinguish different values of N_{ref}. The full connection between F_Q, the asymmetry measures of Marvian and Spekkens [18], and the k-operator resource remains an open problem.

9. The Sector Decomposition Across Clock Types

Part I (§4) [1] establishes that the $1/\gamma$ suppression is clock-independent at the physical level. This section extends the analysis to the k-operator regime, showing that the sector decomposition is universal across physically distinct clock types.

9.1. Light-bounce clock

The light-clock system (mirrors + photon field) has invariant mass M that includes the photon's energy: $M=M_{\text{mirrors}}+\hbar\omega_0/c^2$, where $\omega_0=\pi c/d$ is the cavity mode frequency. The k-operator is:

$$\hat{k}=\frac{\hat{H}_{\text{cm}}+\hat{p}c}{Mc^2}$$

where M is the invariant mass of the composite system, not the bare mirror mass.

The time dilation sector $\hat{k}+\hat{k}^{-1}=2\hat{E}/(Mc^2)$ encodes the nonlinear dependence $E(p)=\sqrt{p^2c^2+M^2c^4}$, which is strictly convex. Jensen corrections and quantum decoherence of the cavity mode under momentum superposition both originate from this nonlinearity.

The simultaneity sector $\hat{k}-\hat{k}^{-1}=2\hat{p}c/(Mc^2)$ is linear and contributes no corrections to the internal oscillation rate under momentum superposition.

The Pikovski expansion may fail for this clock: the photon energy $\hbar\omega_0$ can be comparable to the mirror rest mass for cavity separations on the order of the mirrors' Compton wavelength. However, the budget equation $(d\tau/dt)^2+v^2/c^2=1$ still gives $f=f_0/\gamma$ exactly. The Pikovski route is secondary for the light clock; the budget equation is primary.

The quantum correction magnitude depends on the ratio of photon energy to mirror mass. For a realistic optical cavity with mirror mass $M_{\text{mirror}}\sim 1\,\text{g}$ and cavity photon energy $\hbar\omega_0\sim 1\,\text{eV}$, the Pikovski expansion parameter is $\hbar\omega_0/(M_{\text{mirror}}c^2)\sim 10^{-36}$ and the Jensen correction is negligible. For a hypothetical cavity with mirrors at the Compton wavelength scale, $\hbar\omega_0/(Mc^2)\sim 1$ and the Pikovski expansion fails entirely — but the budget equation still gives $1/\gamma$ exactly.

9.2. Radioactive decay clock

The k-operator for the nucleus uses the nuclear mass m:

$$\hat{k}=\frac{\hat{H}_{\text{cm}}+\hat{p}c}{mc^2}$$

The time dilation sector: $E(p)$ is strictly convex with $d^2E/dp^2=m^2c^6/E^3>0$. Jensen corrections to nuclear transition rates arise from momentum superpositions.

The simultaneity sector: linear in $\hat{p}$, no contribution to decay-rate modification and no decoherence.

The Margolus–Levitin bound is concrete for this clock [17]: $\nu_{\max}\times\gamma=(2/\pi\hbar)(\langle\hat{H}_{\text{nuc}}\rangle-E_0)=\text{const}$. The corrections identified by Grochowski et al. [14] are expected to apply: quantum corrections to nuclear spectra in momentum superpositions should separate by detection geometry.

The quantum correction magnitude $\sigma_p^2/(m_{\text{nuc}}^2c^2)$ is small and not currently observable, but within four orders of magnitude of cold-atom nuclear clock precision, where $\sigma_p/(mc)$ can reach $\sim 10^{-11}$.

For a ^{87}Sr optical lattice clock with nuclear mass $m\approx 87\,\text{u}$ and cold-atom momentum spread $\sigma_p\sim\hbar/\lambda_{\text{lattice}}$ at lattice

wavelength $\lambda_{\text{lattice}} \sim 800\,\text{nm}$, the ratio $\sigma_p/(mc) \sim 10^{-11}$ and the Jensen correction to the time dilation sector is of order 10^{-22} — four orders of magnitude below current precision ($\sim 10^{-18}$), requiring substantial advances in clock comparison sensitivity.

9.3. Gravitational pendulum

The k-operator for the pendulum system uses the total invariant mass M (support structure + bob + oscillation energy):

$$\hat{k} = \frac{\hat{H}_{\text{cm}} + \hat{p}c}{Mc^2}$$

For a macroscopic pendulum, $\sigma_p/(Mc)$ is extraordinarily small. The Jensen correction to the time dilation sector:

$$\langle \hat{k} + \hat{k}^{-1} \rangle = 2\gamma_0 + \frac{\sigma_p^2}{\gamma_0^3 M^2 c^2} + \mathcal{O}(\sigma_p^4)$$

is of order $\sigma_p^2/(M^2c^2) \sim 10^{-60}$ for any macroscopic object. The macroscopic pendulum is deep in the classical limit where all quantum corrections vanish.

For a pendulum of mass $M = 1\,\text{kg}$ at temperature $T = 300\,\text{K}$, the thermal momentum spread is $\sigma_p \sim \sqrt{Mk_BT} \sim 10^{-11}\,\text{kg m/s}$ and $\sigma_p/(Mc) \sim 10^{-20}$, giving a Jensen correction of order 10^{-40}. Even at millikelvin temperatures ($\sigma_p/(Mc) \sim 10^{-23}$), the correction remains at 10^{-46} — permanently unobservable. The macroscopic pendulum confirms the universality of the sector structure while being irretrievably classical in its quantum corrections.

9.4. Universal structure

Table 1 summarizes the sector decomposition across all three clock types.

10. Connection to Pikovski Decoherence

The Pikovski decoherence mechanism [3] — the dephasing of internal clock states due to time dilation — originates entirely from the time dilation sector's nonlinearity. The Bondi decomposition makes this partition explicit.

In a momentum superposition $\sum_i c_i |p_i\rangle$, each momentum component p_i experiences a different value of $1/\gamma(p_i) = mc^2/E(p_i)$. The internal clock phase accumulated over coordinate time T is $\phi_i = \omega_0 T mc^2/E(p_i)$. Since $E(p)$ is nonlinear, distinct momentum components accumulate different phases — this is the dephasing.

The simultaneity sector contributes a deterministic offset $\Delta x_i = p_i cT/(mc^2)$ per component. Since $p \mapsto pc$ is linear, this offset scales uniformly with momentum and produces no relative dephasing between components: $\Delta\phi_{\text{sim}} = 0$.

The Bondi decomposition therefore provides the structural explanation for why the Pikovski mechanism produces decoherence (time dilation sector, nonlinear) rather than a deterministic phase shift (simultaneity sector, linear). This partition is confirmed by the Grochowski spectroscopy of Section 7: the angular signatures of the two sectors correspond to the decoherence-producing and deterministic contributions, respectively.

The decomposition also explains why Pikovski decoherence is universal across clock types (Section 9): the nonlinearity of $E(p)$ is a property of the mass-shell constraint, not of any particular internal Hamiltonian. Every composite system with rest mass $m > 0$ in a momentum superposition will experience the same time-dilation-sector dephasing, with the magnitude set by $\sigma_p/(mc)$.

The Pikovski mechanism fundamentally involves entanglement between internal (clock) and external (momentum) degrees of freedom: distinct momentum components accumulate different internal phases, generating internal-external correlations that reduce the purity of the internal state. The k-operator framework captures the dephasing structure — which sector produces phase spread and which does not — but does not track the entanglement dynamics. A full treatment would require tracing over the momentum degree of freedom to obtain the reduced internal state, connecting the k-operator algebra to the decoherence functional.

11. Discussion

11.1. What the quantum extension establishes

The k-operator decomposition and sector asymmetry are structural results of the mass-shell constraint. The protection of the simultaneity sector by linearity is a theorem, not a contingent fact. Quantum corrections to the Lorentz transformation affect measurement statistics but not the symmetry group: the group property of boosts is a theorem of counting and the relativity principle (Part II, the group-property proposition [2]), and quantum corrections are perturbations around the group-theoretic structure.

The sector decomposition is universal across clock types (Section 9). The clock mechanism determines the magnitude of quantum corrections (through $\sigma_p/(mc)$) but not the structure: which sector produces corrections and which is protected is determined by the mass-shell constraint alone.

The k-operator is not merely an alternative notation for the energy-momentum decomposition. The k-factor $k = N_{\text{received}}/N_{\text{sent}}$ is a physically measurable count ratio — it is the operational content of what two clocks communicating via light signals tell each other. Promoting it to an operator makes the Lorentz transformation the algebra of quantum count ratios, completing the connection between the N_{ref} program of Parts I–II and the quantum regime. The decomposition into $\hat{k} + \hat{k}^{-1}$ (symmetric in send/receive, time dilation) and $\hat{k} - \hat{k}^{-1}$ (antisymmetric, simultaneity) is not an arbitrary algebraic split but the natural partition arising from the radar protocol's $(k, 1/k)$ asymmetry. That this partition simultaneously separates nonlinear from linear momentum dependence — and thereby organizes Jensen corrections, Pikovski decoherence, the Pauli obstruction, and Grochowski angular separation under a single structural cause — is a nontrivial fact about how the mass-shell constraint interacts with the Bondi algebra. The computational content of these results is available in standard notation; what the k-operator provides is the physical grounding that makes the structure visible and the protection of the simultaneity sector immediate.

Property	Light clock	Decay clock	Pendulum
$\hat{H}_0$	Cavity mode	Nuclear Hamiltonian	Mechanical oscillation
Primary route	Budget equation	Pikovski	Budget equation (via EP)
$\sigma_p/(mc)$	Depends on cavity	$\sim 10^{-11}$ (cold atoms)	$\sim 10^{-30}$
Jensen correction	$\sim 10^{-36}$ (realistic); large only at Compton scale (hypothetical)	Small but detectable	$\sim 10^{-60}$
Simultaneity correction	Zero	Zero	Zero

Table 1: The k-operator sector decomposition across three clock types. The clock type determines the magnitude of quantum corrections (through $\sigma_p/(mc)$). The structure — which sector contributes corrections and which is protected — is universal.

11.2. Connection to the surplus structure program

Parts I and II [1, 2] establish that the temporal parameter $t \in \mathbb{R}$ carries surplus structure (in Weatherall's sense [15]; see also Gisin [16] for the antecedent observation that the mathematical language used to model time shapes what physics can express). This paper shows that when the framework is extended to quantum clocks, the surplus structure claim remains intact: quantum corrections appear in the time-dilation sector (through Jensen's inequality) but the total constraint structure is unchanged.

No quantum correction introduces new surplus structure beyond what was identified in Part I. The three surplus properties of $\mathbb{R}$ (negative extension, loop-admitting topology, reversal symmetry) are absent from the quantum k-operator framework in the same way they are absent from the classical Bondi derivation.

The quantum corrections of this paper operate at both levels identified in Part I (§8.6) [1]: they modify the local N_{ref} tick rate (time dilation sector, Jensen corrections) and the coordination-layer parameter constructed from those rates (measurement statistics of the Lorentz transformation, Section 4.3).

11.3. Experimental prospects

The sector decomposition organizes three experimentally distinguishable signatures, each already discussed in the literature:

Grochowski spectroscopy [14]: detection-angle separation of the two sectors in atomic spectra. Perpendicular detection ($\Theta = \pi/2$) isolates the time dilation sector; parallel detection ($\Theta = 0$) is dominated by the simultaneity contribution.

Covey–Pikovski–Borregaard [19]: a distributed quantum clock network designed to probe quantum dynamics in curved geometry beyond the Newtonian limit. The precision threshold at which the sector decomposition produces observable signatures is at corrections of order $\sigma_p^2/(m^2c^2)$, which would become detectable at cold-atom temperatures given sufficient precision improvements.

Cold-atom regime. The most promising near-term platform is cold-atom interferometry, where $\sigma_p/(mc) \sim 10^{-11}$ for optical-lattice-trapped atoms. The Jensen correction to the time dilation sector at this scale is $\sigma_p^2/(m^2c^2) \sim 10^{-22}$, four orders of magnitude below current optical clock precision ($\sim 10^{-18}$). Reaching this threshold would require either a four-order-of-magnitude improvement in clock comparisons or an amplification scheme that accumulates the correction over many cycles. The Grochowski angular separation provides an alternative detection strategy that does not require absolute frequency comparisons.

11.4. Open problems

Higher-order corrections and non-Gaussian states. The Jensen correction is the leading order in $\sigma_p^2/(m^2c^2)$. Higher-order corrections for non-Gaussian momentum distributions have not been computed.

Gravitational extension. Whether the k-operator sector decomposition persists under gravitational corrections — specifically, whether the simultaneity sector remains linear in p in curved spacetime — is open (the gravitational-extension open question of Part II [2]). Favalli and Smerzi [11] provide a recent analysis of quantum clock time dilation in a relativistic gravitational potential that may constrain this extension.

Fully quantum signal. The Bondi derivation uses classical light signals. A fully quantum treatment using single-photon Fock states would test whether the k-factor extraction survives when the signal itself is quantum.

Marvian–Spekkens connection. The full connection between the QFI criterion (Proposition 8.1), the asymmetry measures of Marvian and Spekkens [18], and the k-operator resource theory remains open.

12. Conclusion

Part I establishes that the full Lorentz transformation is derivable from count-based primitives. Part II provides the axiomatic and categorical foundations, including the counting axioms (N1–N4), the categorical surplus identification, and the signature theorem. This paper asks: what happens when the clocks are quantum?

The k-factor becomes an operator, and the two sectors of the Lorentz transformation acquire structurally different quantum-correction profiles. The time dilation sector ($\hat{k} + \hat{k}^{-1}$), being nonlinear in momentum through the mass-shell constraint, produces Jensen corrections, Pikovski decoherence, and the Pauli obstruction. The simultaneity sector ($\hat{k} - \hat{k}^{-1}$), being linear in momentum, is protected from all three. The root cause is rest mass $m > 0$, which bounds the energy spectrum below and makes $E(p)$ strictly convex.

The decomposition is universal across physically distinct clock types: light-bounce, radioactive decay, and gravitational pendulum clocks all exhibit the same sector

structure, with the magnitude of quantum corrections determined by $\sigma_p/(mc)$ and the structural partition determined by the mass-shell constraint alone. The two sectors produce experimentally distinguishable signatures in atomic spectroscopy, separable by angular detection geometry.

All corrections vanish in the classical limit $\sigma_p \to 0$, recovering the Bondi derivation of Part I exactly. The surplus structure claim of Parts I and II remains intact under the quantum extension: no quantum correction introduces new surplus structure beyond what was identified in the classical framework.

Declarations

Funding. This research received no external funding.

Competing interests. The author declares no competing interests.

Data availability. No datasets were generated or analysed during the current study. All results are derived analytically from the k-operator algebra developed in the text; the schematic figures are illustrative and contain no underlying data.

Use of AI tools. The author used Claude (Anthropic) for editorial assistance during manuscript preparation, including copy-editing, validation of internal cross-references, and consistency checking across the three-paper series. All scientific content, mathematical derivations, and arguments are the author's own. The author takes full responsibility for the content of the publication.

References

[1] B. Rajagopalan, Surplus Structure in the Temporal Parameter: Consequences of the Mass-Shell Constraint and the N_{ref} Substitution, Part I of three, preprint (2026).

[2] B. Rajagopalan, Counting Axioms for the Temporal Parameter: Axiomatic and Categorical Foundations of the N_{ref} Framework, Part II of three, preprint (2026).

[3] I. Pikovski, M. Zych, F. Costa, and Č. Brukner, Universal decoherence due to gravitational time dilation, *Nature Physics* **11**, 668 (2015).

[4] A.R.H. Smith and M. Ahmadi, Quantum clocks observe classical and quantum time dilation, *Nature Communications* **11**, 5360 (2020).

[5] P.A. Höhn, A.R.H. Smith, and M.P.E. Lock, Trinity of relational quantum dynamics, *Phys. Rev. D* **104**, 066001 (2021).

[6] P.A. Höhn, A.R.H. Smith, and M.P.E. Lock, Equivalence of approaches to relational quantum dynamics in relativistic settings, *Frontiers in Physics* **9**, 587083 (2021).

[7] D.N. Page and W.K. Wootters, Evolution without evolution: Dynamics described by stationary observables, *Phys. Rev. D* **27**, 2885 (1983).

[8] H. Bondi, *Relativity and Common Sense*, Heinemann (1964).

[9] A. Vanrietvelde, P.A. Höhn, F. Giacomini, and E. Castro-Ruiz, A change of perspective: switching quantum reference frames via a perspective-neutral framework, *Quantum* **4**, 225 (2020).

[10] A. Vanrietvelde, P.A. Höhn, and F. Giacomini, Switching quantum reference frames in the N-body problem and the absence of global relational perspectives, *Quantum* **7**, 1088 (2023).

[11] T. Favalli and A. Smerzi, Time dilation of quantum clocks in a relativistic gravitational potential, *Entropy* **27**(5), 489 (2025).

[12] W. von Ignatowsky, Einige allgemeine Bemerkungen zum Relativitätsprinzip, *Phys. Zeitschr.* **11**, 972 (1910).

[13] V. Berzi and V. Gorini, Reciprocity Principle and the Lorentz Transformations, *J. Math. Phys.* **10**, 1518 (1969).

[14] P.T. Grochowski, A.R.H. Smith, A. Dragan, and K. Dębski, Quantum time dilation in atomic spectra, *Phys. Rev. Research* **3**, 023053 (2021).

[15] J.O. Weatherall, Understanding Gauge, *Philosophy of Science* **83**, 1039 (2016).

[16] N. Gisin, Mathematical languages shape our understanding of time in physics, *Nature Physics* **16**, 114 (2020).

[17] N. Margolus and L.B. Levitin, The maximum speed of dynamical evolution, *Physica D* **120**, 188 (1998).

[18] I. Marvian and R.W. Spekkens, Extending Noether's theorem by quantifying the asymmetry of quantum states, *Nature Communications* **5**, 3821 (2014).

[19] J.P. Covey, I. Pikovski, and J. Borregaard, Probing curved spacetime with a distributed atomic processor clock, *PRX Quantum* **6**, 030310 (2025).

[20] W. Pauli, Die allgemeinen Prinzipien der Wellenmechanik, in *Handbuch der Physik*, Vol. 24, Part 1, Springer, Berlin (1933).